



Short communication

Late steps of parvoviral infection induce changes in cell morphology

Kirsi Pakkanen*, Jonna Nykky, Matti Vuento

Department of Biological and Environmental Science and Nanoscience Center, P.O. Box 35, University of Jyväskylä, FIN-40014 Jyväskylä, Finland

ARTICLE INFO

Article history:

Received 18 May 2008

Received in revised form 9 July 2008

Accepted 11 July 2008

Available online 5 September 2008

Keywords:

Canine parvovirus

Extension

Egress

Host cell morphology

ABSTRACT

Previously, virus-induced non-filopodial extensions have not been encountered in connection with viral infections. Here, we report emergence of long extensions protruding from Norden laboratory feline kidney (NLFK) and A72 (canine fibroma) cells infected with canine parvovirus for 72 h. These extensions significantly differ in length and number from those appearing in control cells. The most striking feature in the extensions is the length, reaching up to 130 μm , almost twice the average length of a healthy NLFK cell. In A72 cells, the extensions were even longer, up to 200 μm . The results presented here also suggest that the events leading to the growth of these extensions start earlier in infection and abnormal extension growth is detectable already at 24-h post-infection (p.i.). These extensions may have a vital role in the cell-to-cell transmission of the virus.

© 2008 Elsevier B.V. All rights reserved.

To ensure an efficient way of exit from host cells, some viruses utilize host-cell cytoskeleton for transport, not only to reach the plasma membrane but also to spread from one cell to another. One of the classical examples of cytoskeleton-mediated exit of virus particles is the actin-tail propelling of vaccinia virus (Cudmore et al., 1995). Recently, also virus-induced formation of cellular filopodia has been reported (Sherer et al., 2007). Murine leukemia virus, a retrovirus, has been shown to induce filopodia-growth from uninfected cells, protruding towards the infected cells to form means of cell–cell transfer for the virus (Sherer et al., 2007). Filopodia growth has also been observed in cells transfected with Semliki Forest virus (SFV) and Sindbis virus virus-specific nonstructural proteins (Laakkonen et al., 1998). Filopodial actin bundles have also been associated with the release of Marburgvirus particles (Kolesnikova et al., 2007).

In contrast to filopodia, alphaherpesviruses herpes simplex virus (HSV) and porcine pseudorabies virus induce long projections in their host cells. These, in the case of HSV have been measured to extend up to 100 μm outwards (Boissière et al., 2004; Favoreel et al., 2005). Long neurite-like extensions in fibroblasts have been observed with simultaneous inhibition of Rho-effector ROCK and the multiadaptor proto-oncoprotein Cbl (Scaife et al., 2003). Cellular extensions have also been shown to have importance in viral entry. For example, in a recent study vaccinia virus was shown to move along host cell filopodia before being internalized into the cell (Mercer and Helenius, 2008).

Canine parvovirus (CPV) is a member of the autonomous Parvovirus genus of the Parvoviridae family (Tattersall and Cotmore, 1988). CPV is a small, non-enveloped virus, the virus capsid having a diameter of approximately 26 nm (Chapman and Rossmann, 1993). CPV enters into its host cells via transferrin receptors and clathrin-mediated endocytosis (Parker et al., 2001; Suikkanen et al., 2002). During its entry, CPV utilizes the microtubule network of the host cell to advance towards the nucleus, following release from endosomal vesicles. By using dynein-dependent traffic along the microtubules, CPV bypasses the steric obstacles and the high viscosity of the cytoplasm, which hinder diffusion inside the cell. Also, CPV has been shown to interact with microtubules in vitro (Suikkanen et al., 2003).

While the entry phase of CPV life cycle is characterized in detail, there is little information on the late steps of the infection in host cells. Here, we report that in CPV infection lasting for 72 h, long extensions protrude from the host cells, reaching up to 130 μm . The number and the length of these extensions differed significantly from those of the uninfected control. This suggests the extensions to be virus-induced and may therefore contribute to the egress mechanism of the virus.

Both cell lines, Norden laboratory feline kidney (NLFK) cells and canine fibroma A72 cells were grown and maintained in Dulbecco's modified Eagle's medium (PAA Laboratories GmbH, Pasching, Austria) supplemented with 10% fetal calf serum (PAA Laboratories GmbH). CPV derived originally from the infectious plasmid clone of the virus (Parrish, 1991) was cultured and purified as previously described (Suikkanen et al., 2002). For infection experiments, the cells were grown to a 90% confluency on glass coverslips and infected with approximately 2×10^9 CPV particles. CPV infection is deleterious for cells and during the 72 h infection cells already start

* Corresponding author. Tel.: +358 14 260 4228; fax: +358 14 260 4756.
E-mail address: kiinpakk@byti.jyu.fi (K. Pakkanen).

to detach from the glass surface. To prevent the longer intercellular distance arising from this to affect the results, the control cells for 72 h infection studies were grown at a 50% confluency before the start of the 72 h control period.

At appropriate time points cells were fixed with ice-cold methanol (Sigma–Aldrich, St. Louis, MO). For immunofluorescence labeling, the samples were blocked with 3% bovine serum albumin (Sigma–Aldrich) and labeled with antibodies using standard protocols. To prevent cross-reaction between the two primary mouse antibodies used, the antibodies were used in pairs of primary and secondary antibody, and an additional blocking step was applied between the first secondary and second primary antibody. Mouse monoclonal antibody to the CPV capsid (Mab8, (Strassheim et al., 1994)) and mouse monoclonal antibody to alpha-tubulin (Sigma–Aldrich) were used as primary antibodies and Northern Lights donkey anti-mouse NL-557 (R&D Systems Inc., Minneapolis, MN) and Alexa Fluor 488 conjugated anti-mouse antibody (Molecular Probes, Eugene, OR) as secondary antibodies. The nuclei were stained with Hoechst 33342 (Sigma–Aldrich) to assess cell viability. Infection experiments with A72 cells for extension quantification were imaged using unstained, live cells on coverslips. The samples were imaged using a confocal microscope (LSM510, Zeiss Axiovert 100M, Jena, Germany). Apart from Fig. 1 J, all fluorescence images are presented scaled to intensity so that blue colors present lower and green colors higher intensity. Intensity coloring was made using ImageJ software (Rasband, W.S., ImageJ, U.S. National Institutes of Health, Bethesda, MD, USA).

Quantification of cell extension length was performed with ImageJ software using difference interference contrast (DIC) images. Calculations of the extension number per cell was manually performed. Kruskal–Wallis analysis was used to calculate the total variance between groups and Mann–Whitney *U*-test with Bonferroni–Holm correction for pairwise comparisons (** $P < 0.05$, *** $P < 0.005$). Statistical analyses were made using Kaleidagraph software (Synergy Software, Reading, PA).

The morphology of CPV-infected NLFK and A72 cells was analyzed by DIC imaging. The NLFK cells, flat and characteristically triangular in control culture, bore no clear differences at 24-h post-infection (p.i.). However, by 72-h p.i. the morphology of the cells had profoundly changed (Fig. 1 A, C, E and G). Similar morphological changes were visible also with the A72 cells after 72 h of infection (not shown). The body of the cells had become rounder, yet the cells were not detached from the cover slips. More importantly, the cells had developed long protrusions, reaching up to 130 μm in case of NLFK cells and 200 μm in case of A72 cells. In addition, in some cases the extensions were detected fusing with neighboring cells or protrusions of neighboring cells. Although the cell body roundness and the protrusions of the cells could also be detected in uninfected control cells grown at subconfluency for 72 h, these features were strikingly more pronounced in infected cells for both of the studied cell lines. Also, at 72-h p.i. smaller filopodia-like extensions were apparent in NLFK cells (Fig. 1I) as well as in A72 cells (not shown). Based on staining with Hoechst 33342, some of the NLFK cells at 72-h p.i. were undergoing apoptosis or necrosis, but the presence of extensions did not correlate with the anomalous staining with Hoechst 33342 (data not shown).

Visualizing NLFK cells with immunofluorescence methods using tubulin antibody revealed again long protrusions in cells at 72 h, and similar to the DIC imaging, shorter extensions could be observed in control cells grown for 24 or 72 h (Fig. 1 B, D, F and H). No significant contribution of actin or vimentin were found in the extensions (data not shown). It was also of notice, that the pattern of tubulin organization and the intensity of the tubulin-label differed in infected cells when compared with the uninfected control. In cells infected for 24 h, tubulin was localized mostly on the

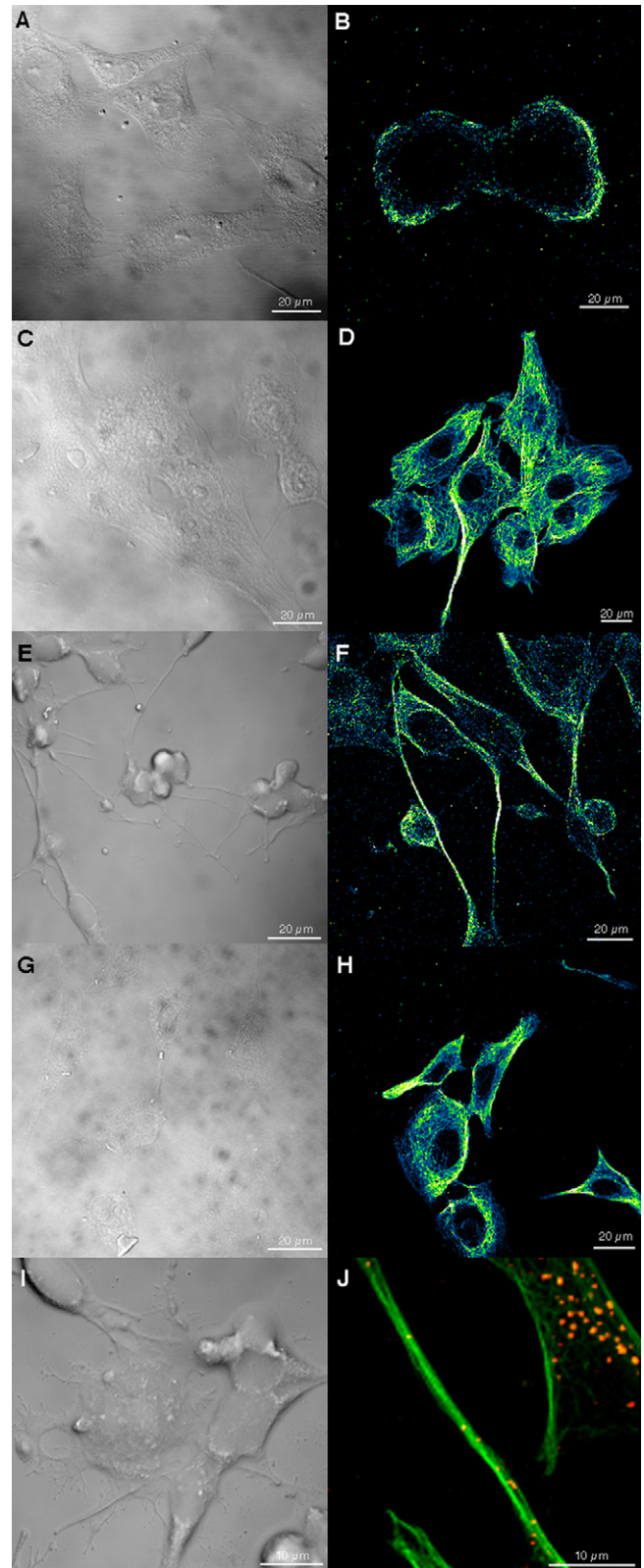


Fig. 1. Formation of neurite-like extensions during CPV infection. Differential interference contrast (DIC) image (A) and anti-tubulin labeling (B) of CPV-infected NLFK cells at 24-h post-infection (p.i.). DIC image (C) and anti-tubulin labeling (D) of control cells grown for 24 h. DIC image (E) and anti-tubulin labeling (F) of infected cells at 72-h p.i. DIC image (G) and anti-tubulin labeling (H) of control cells grown for 72 h. In figures B, D, F and H blue presents lower intensity of fluorescence and green higher intensity. Smaller, filopodia-like protrusions of cells 72-h p.i. (I). Co-labeling of tubulin (green) and CPV capsids (red) (J).

Download English Version:

<https://daneshyari.com/en/article/3430162>

Download Persian Version:

<https://daneshyari.com/article/3430162>

[Daneshyari.com](https://daneshyari.com)